Current transport mechanisms in GaAs/AlAs tunnel structures grown by metal–organic chemical vapor deposition

A. R. Bonnefoi, D. H. Chow, and T. C. McGill
T. J. Watson, Sr., Laboratory of Applied Physics, California Institute of Technology, Pasadena, California 91125

R. D. Burnham and F. A. Ponce
Xerox Corporation, Palo Alto, California 94304

(Received 5 March 1986; accepted 7 April 1986)

Elastic and inelastic tunneling processes are investigated in GaAs–AlAs–GaAs double heterojunctions grown in the [100] direction by metal–organic chemical vapor deposition (MOCVD). The AlAs quantum barriers in the heterostructures studied are doped p-type with Mg. Theoretical calculations of tunneling currents are performed and compared with experimental I–V data. It is found that for structures with thin AlAs barriers, the dominant current transport mechanism at low temperatures is tunneling through the AlAs band gap at both the Γ and X points. This is consistent with inelastic processes observable in first (dI/dV) and second (d^2I/dV^2) derivative spectra obtained with modulation techniques. A simple model, developed for calculating impurity-assisted tunneling currents, shows that the role of barrier impurities becomes more important as the barrier is grown thicker. Implications of some of these results for resonant tunneling heterostructures consisting of two AlAs quantum barriers separated by a GaAs quantum well are discussed. Experimental second derivative spectra showing reproducible features are also presented for these double barrier structures.

I. INTRODUCTION

Because of their numerous potential device applications, semiconductor quantum well and quantum barrier heterostructures are the object of considerable theoretical and experimental work. These structures are frequently fabricated from GaAs and $Al_xGa_{1-x}As$, using techniques such as molecular beam epitaxy (MBE) and metal–organic chemical vapor deposition (MOCVD) to achieve small characteristic dimensions. In structures with thin quantum barriers, an important current transport mechanism is electron tunneling. Several studies of electronic transport in single and double barrier tunnel structures have been reported.[1–10] The associated tunneling effects yield novel electronic properties, some of which remain to be fully understood. Most of the studies to date, both theoretical and experimental, have used $Al_xGa_{1-x}As$ quantum barriers in which the Al composition, x, was small enough that the alloy was still direct.[5–10] Furthermore, most of the experimental investigations have been performed on MBE grown wafers.[4–8] Only a few studies have been reported on MOCVD grown samples,[1–3] and/or structures in which the barriers consisted of indirect $Al_xGa_{1-x}As$,[3,4] or pure AlAs.[1,2]

In this paper, we concentrate primarily on current transport mechanisms at low temperatures in GaAs–AlAs–GaAs double heterojunctions grown by MOCVD in the [100] direction. In Sec. II, we briefly present the sample growth and preparation procedures. In Sec. III, we report both experimental and theoretical results for structures with thin p-type AlAs barriers. We first calculate current–voltage (I–V) characteristics at low temperatures due to elastic tunneling through the AlAs band gap at the Γ point, using the actual shape of the barrier obtained from band bending calculations. Upon comparing the calculated and experimental I–V curves, it is found that tunneling through the AlAs Γ-point barrier fails to explain the experimental data. This indicates that other transport mechanisms must contribute to the total current. Tunneling through the AlAs band gap at the X point is then discussed. Good theoretical fits of the experimental I–V data can be obtained by considering tunneling through both the Γ- and X-point barriers. In Sec. IV, we introduce a new element to the calculation of the theoretical I–V curves: the presence of trap levels in the AlAs band gap, due to defects or impurities. A simple model is developed to calculate the impurity-assisted tunneling current. This current becomes more important as the quantum barriers become thicker, and can actually become the dominant current transport mechanism through thick enough barriers. In Sec. V, implications of some of these results for resonant tunneling heterostructures made of two AlAs quantum barriers separated by a GaAs quantum well are discussed. For these structures, experimental derivative spectra showing reproducible and periodic features are also reported. Finally, the results of the present study are summarized in Sec. VI.

II. EXPERIMENTAL PROCEDURES

The samples used in this study were grown by an MOCVD technique[11,12] on a [100]-oriented GaAs substrate doped n-type with Si at $2–3\times10^{18}$ cm^{-3}. A first epitaxial layer of degenerate GaAs, doped n-type with Se, was grown 2–3 μm thick. In single barrier structures, this layer was followed first by an AlAs layer doped p-type with Mg,[13,14] and then by another GaAs layer, degenerately doped with Se. Samples were grown with GaAs dopings ranging between 1×10^{18} and 5×10^{18} cm^{-3}, AlAs barrier thicknesses between 40 and 250 Å, and barrier dopings estimated to vary between 1×10^{17} and 3×10^{18} cm^{-3}. In dou-

 0734-211X/86/040988-08$01.00

ble barrier structures, the first epitaxial GaAs layer was followed by two thin AlAs layers separated by a quantum well of nominally undoped GaAs. The AlAs barriers were doped p-type with Mg at approximately 1×10^{18} cm^{-3}. Finally, a GaAs top layer was grown, degenerately doped with Se. The thicknesses of the AlAs barriers and the GaAs wells were determined by transmission electron microscopy (TEM). Electrode dopings were obtained from Polaron doping profiles. Barrier dopings were estimated from the flow rates used during growth. They could thus be in error due to the difficulty of accurately calibrating dopings in such thin layers.

Devices were made by defining mesas on the epitaxial sample face using conventional photolithography and a GaAs etch (4:1:1, H_2SO_4:H_2O_2:H_2O). The mesas were circular and 50–700 μm in diameter. Ohmic contacts were made on the surface of the mesas and on the substrate by evaporating Au–Ge, or Au–Ge, Ni, Au, and then annealing at 380–410 °C for 20–30 s.

Measurements of current–voltage curves (I–V), as well as first (dI/dV) and second (d^2I/dV^2) derivatives of the I–V curves were performed at temperatures ranging from 300 to 4.2 K. The I–V curves were measured with an HP 4145 semiconductor parameter analyzer. The first and second derivative spectra were obtained using modulation techniques at 5 and 50 kHz, respectively.

III. RESULTS ON THIN SINGLE BARRIER STRUCTURES

In this section, we present both experimental and theoretical results for single barrier heterostructures having a thin AlAs barrier layer totally depleted of carriers. A number of studies have reported that the dominant current transport mechanism at low temperatures in $Al_xGa_{1-x}As$ quantum barrier structures is elastic tunneling through the $Al_xGa_{1-x}As$ direct band gap at the Γ point.[3,5,6] In these studies, theoretical I–V curves were calculated assuming a trapezoidal shape for the quantum barrier under applied bias, and compared to experimental data on logarithmic scales. Nevertheless, discrepancies were observed[5] which indicated that other current transport mechanisms can compete with elastic Γ-point tunneling. Theoretical studies have also reported that Γ-point electrons in the GaAs electrodes should tunnel through the $Al_xGa_{1-x}As$ band gap at the Γ point even in indirect alloys.[15,16] However, we show here that experimental data for structures with pure AlAs barriers cannot be explained by Γ-point tunneling alone. We propose that there is a small, but nonnegligible probability that the incident electrons tunnel through the AlAs X-point barrier.

Current densities are calculated using the following approach. First, the actual shape of the conduction band edge in the electrodes and the barrier is determined from band bending calculations. These calculations are found to be of critical importance, particularly in samples with heavily doped barriers. They are performed by solving Poisson's equation self-consistently throughout the entire heterostructure at each applied voltage. The transmission coefficient for tunneling electrons is then calculated using the WKB approximation. The attenuation constant in the barrier is determined from a two-band model, $\mathbf{k}\cdot\mathbf{p}$ theory formula[17] for electrons tunneling through the AlAs Γ point, and a simple "one-band model" formula for electrons tunneling through the AlAs X point. Finally, the current density, J, is calculated as a function of applied voltage, V, using the approach of Tsu and Esaki.[9]

Although our study was performed on a wide selection of samples and at temperatures ranging from 300 to 4.2 K, we only illustrate the most important results by discussing data obtained at low temperatures from a single barrier structure having a thin p-type AlAs barrier layer. A more detailed report, including results for heterostructures with n-type AlAs barriers, will be presented in a forthcoming publication.

In the structure of interest, the GaAs electrodes are doped n-type with Se at $4–5\times10^{18}$ cm^{-3}. The doping in the p-type AlAs barrier layer is estimated to be on the order of 10^{18} cm^{-3}. A barrier thickness of 48 Å was obtained from TEM measurements, accurate to within one monolayer. Figure 1 shows the calculated conduction band edge of the structure at the Γ and X points as a function of distance in the direction perpendicular to the plane of the layers. Figure 1(a) depicts thermal electronic equilibrium while Fig. 1(b) corresponds to an applied bias of 200 mV. In the band bending calculations, the dopings in the n-type GaAs electrodes and the p-type AlAs barrier are taken to be 4×10^{18} and 3×10^{18} cm^{-3}, respectively. The barrier thickness is 48 Å. The calculations are performed assuming a temperature of 0 K. The values of the band offsets are key parameters in determining the shape of the barriers seen by the tunneling electrons. These values are still a matter of debate. In a recent experimental study, Batey *et al.*[18] obtained a valence band discontinuity of 0.55 eV in GaAs–AlAs heterostructures. Using this result, values close to 190 meV and 1.04 eV can be calculated for the conduction band offsets at the X and Γ points, respectively. It should be noted that when such values are used, the X-point conduction band edge lies at higher energies in GaAs than in AlAs. This is illustrated in Fig. 1, with the solid line corresponding to the Γ-point conduction band edge and the dashed line to the X-point conduction band edge. Figure 1(a) shows that the barrier is totally depleted of carriers and that the effect of band bending is to increase the average barrier height seen by the tunneling electrons. This effect increases with barrier doping and thickness. In Fig. 1(b), a voltage of 200 mV is applied across the structure. This voltage alters the shape of the conduction band edge in the cladding layers as well as in the barrier. This is another essential factor in calculating tunneling currents. In Fig. 2, we show the experimental characteristic, $J_{exp}(V)$, at 4.2 K in the voltage range 0–200 mV and, on the same linear scale, the calculated current density, $J^{\Gamma}_{el}(V)$, for elastic Γ-point tunneling. Since the structure is symmetric, the J–V curves are symmetric with respect to the origin and we only show the forward bias direction. The two curves are in good agreement at very low biases ($\leqslant$20 mV), but start to deviate significantly in magnitude and shape at higher voltages. While J^{Γ}_{el} varies almost linearly with voltage, the experimental cur-

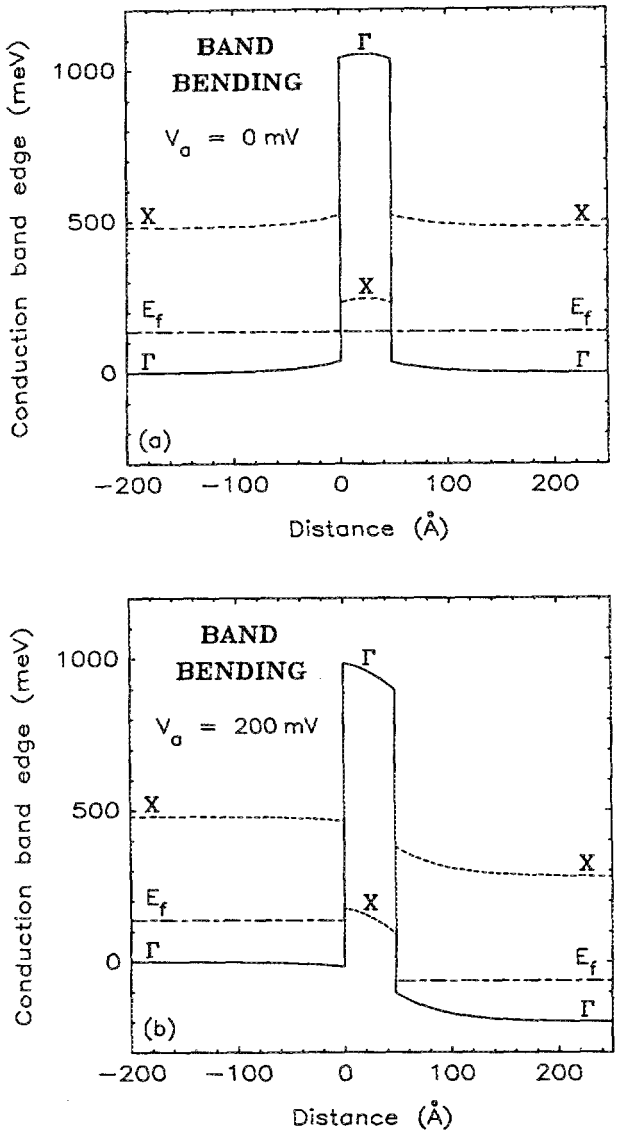

FIG. 1. Calculated conduction band edge at the Γ point (solid line) and at the X point (dashed line), as a function of distance in the direction perpendicular to the plane of the layers, for a GaAs–AlAs–GaAs single barrier heterostructure. The GaAs electrodes are doped n-type at 4×10^{18} cm^{-3}. The AlAs barrier is 48 Å thick and doped p-type at 3×10^{18} cm^{-3}. The conduction band discontinuities at the X and Γ points are 190 meV and 1.04 eV, respectively. (a) Corresponds to thermal electronic equilibrium, and (b) to an applied voltage of 200 mV. The solid–dashed lines correspond to the Fermi level, E_f, in the electrodes. The temperature is assumed to be 0 K.

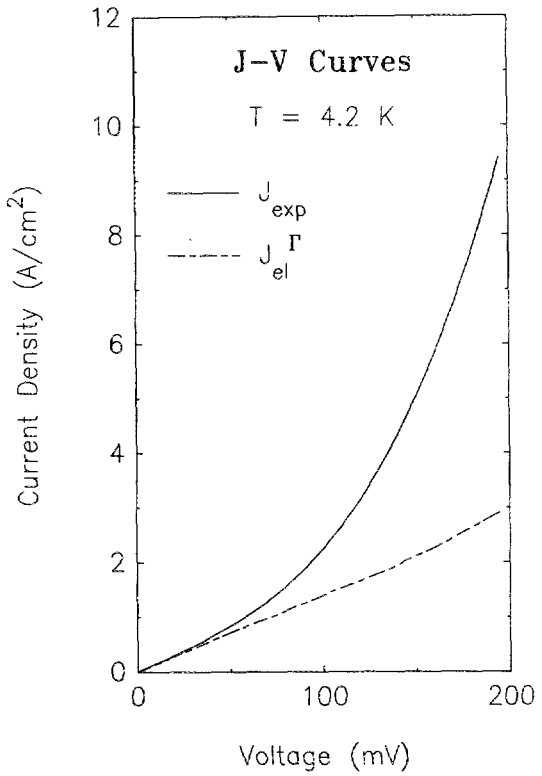

FIG. 2. Experimental and theoretical current–voltage characteristics for the single barrier structure shown in Fig. 1. The solid line corresponds to the experimental current density, J_{exp}. The dashed line is the calculated Γ-point elastic current density, J_{el}^{Γ}.

rent density, J_{exp}, displays a nearly exponential voltage dependence. Similar discrepancies between experimental and theoretical data are observed in all of our samples. This is a clear indication that elastic tunneling through the AlAs band gap at the Γ point does not account for all of the experimental current and that other transport mechanisms are present. These observations are further supported by derivative spectra which reveal threshold voltages for impurity-assisted and/or inelastic tunneling processes. This is illustrated in the second derivative curve, $(d^2I/dV^2)(V)$, shown in Fig. 3. This spectrum displays two prominent and broad features, labeled (a) and (b), peaked at approximately 20 and 80 mV. It also reveals two narrower peaks at about 37 and 50 mV. These have been attributed previously to electron-optical phonon coupling in the GaAs electrodes, and the excitation of longitudinal optical (LO) phonons in the AlAs barrier, respectively.[1] Leakage has been eliminated as a possible source of current by verifying that the experimental J–V curves were reproducible and independent of device area. The behavior of the Γ-point elastic current can easily be understood in terms of the complex band structure of AlAs: In the band gap, the imaginary part of the complex wave vector at the Γ point varies very slowly with energy, except near the conduction and valence band edges. This is due to the small Γ-point effective mass. Therefore, because of the large conduction band offset ($\approx$1 eV), the Γ-point current remains slowly varying with voltage up to about 0.8 V.

In order to tentatively explain the discrepancies between experimental J–V data and calculated Γ-point elastic tunneling currents, a number of transport mechanisms can be suggested. The simplest is the emission of phonons or the excitation of collective modes by electrons tunneling through the AlAs Γ-point barrier. Although some of these inelastic processes may be resolved in derivative spectra, they yield currents which are typically at least two or three orders of magnitude smaller than elastic currents, and therefore too small to account for the observed discrepancies. Another possible current transport mechanism is tunneling via energy levels in the AlAs band gap or at the GaAs/AlAs interfaces. A simple model for impurity-assisted tunneling is developed in Sec. IV. Assuming that no impurity bands or clusters are

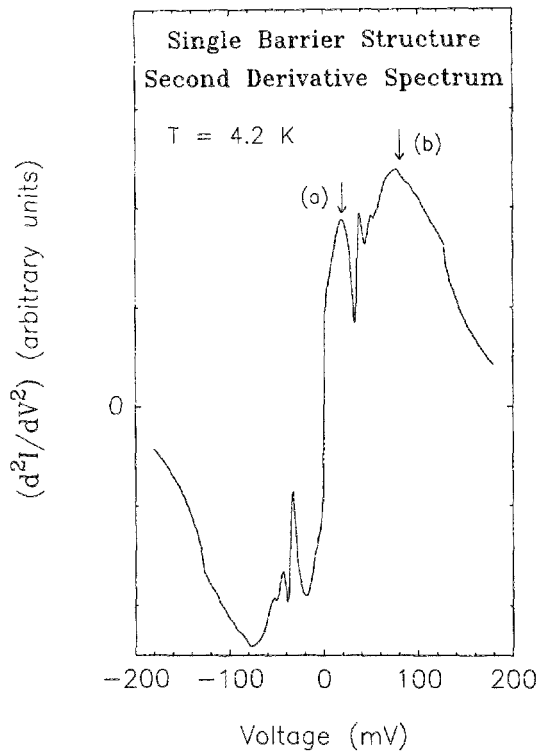

FIG. 3. Experimental second derivative spectrum $(d^2I/dV^2)(V)$, at 4.2 K for the single barrier heterostructure illustrated in Fig. 1. The two most prominent peaks labeled (a) and (b) may correspond to inelastic processes by which GaAs Γ-point electrons scatter into AlAs X-point states. The two narrower peaks at 37 and 50 mV have been attributed previously to electron-optical phonon coupling in the GaAs electrodes, and the excitation of longitudinal optical (LO) phonons in the AlAs barrier, respectively (Ref. 1).

formed, this mechanism gives negligible current densities for the 48 Å barrier structure considered here. Another possibility is to take into account tunneling through the AlAs band gap at symmetry points other than the Γ point. In the case of epitaxial growth in the [100] direction, an important contribution could come from the AlAs X-point valleys. For electrons tunneling from left to right, new channels open when the Fermi level in the left electrode and the X-point conduction band edge in the right electrode align. However, such processes can only occur at voltages $\geqslant$350 meV in the structure discussed here. This is again in disagreement with experimental data. Other mechanisms can allow electrons occupying Γ-point states in both GaAs electrodes to tunnel through the AlAs X-point barrier. Two such processes are discussed below.

First, Γ-point electrons near the GaAs–AlAs interface may scatter inelastically into virtual states beneath the four AlAs X valleys lying along the k_y and k_z directions, parallel to the plane of the layers. They may then tunnel through the AlAs band gap at the X point, and scatter again, near the AlAs–GaAs interface, into the Γ valley in the right electrode. Since electrons travel along the x axis, perpendicular to the plane of the layers, the effective mass in the barrier is the small transverse effective mass $m_t^* = 0.19m_e$, where m_e is the free electron mass. Such inelastic processes, which require two scattering events, can occur through a number of mechanisms such as phonon scattering, for example. Calculations of scattering matrix elements and current densities are being performed to determine which of these processes may explain the experimental data. The matrix elements can be complicated functions of the scattering mechanism, applied voltage, structure characteristics, electron energy, and temperature. In the present study, we simply assume that there is a small probability that incident electrons tunnel through the AlAs band gap at the X point and that the scattering matrix element for a given process is constant. The calculated current density for any such mechanism thus contains an empirical factor, B_{in}. Threshold voltages for these inelastic processes are chosen to coincide with some of the most prominent peaks observed in experimental second derivative spectra $(d^2I/dV^2)(V)$. The total theoretical current density, $J_{th}(V)$, is then calculated by summing the contributions from Γ-point elastic tunneling and X-point inelastic tunneling. Figure 4 is a plot of J_{th} as a function of applied voltage for the structure discussed here. Only two inelastic processes are used to calculate the X-point inelastic tunneling current. These two processes are assigned threshold voltages of 20 and 80 mV, and empirical B_{in}'s of 0.6×10^{-4} and 1.3×10^{-4}, respectively. The threshold voltages correspond to the two most prominent peaks labeled (a) and (b) in the second derivative curve illustrated in Fig. 3. Since two scattering events are required to allow electrons to tunnel through the AlAs X-point barrier, peaks should be observed

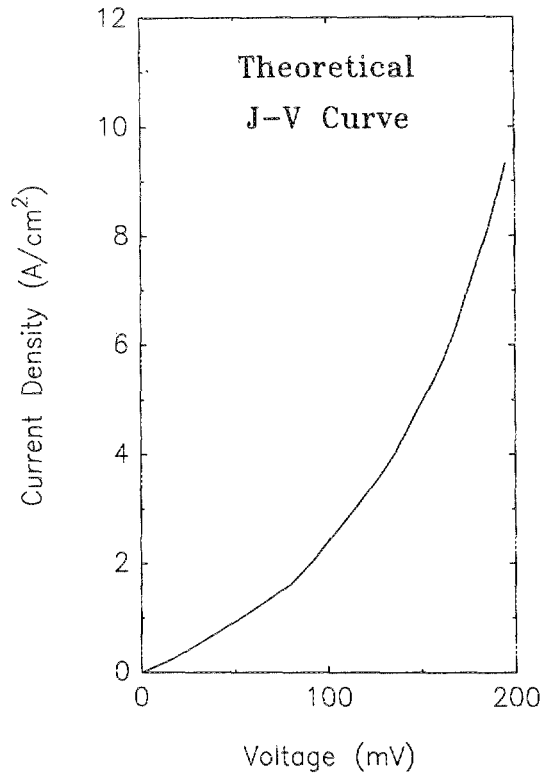

FIG. 4. Total theoretical current density, J_{th}, obtained by summing the contributions of Γ-point elastic tunneling and two X-point inelastic tunneling mechanisms, for the same single barrier structure as in Fig. 2. For the inelastic processes, threshold voltages of 20 and 80 mV are taken in agreement with experimental second derivative (d^2I/dV^2) data. The corresponding empirical B_{in}'s are 0.6×10^{-4} and 1.3×10^{-4}, respectively.

in the $(d^2I/dV^2)(V)$ spectra at voltages corresponding to the sum of the two scattering energies. Peak (a) would thus be consistent with the inelastic excitation of two X-point transverse acoustic (TA) phonons. On the other hand, the broad peak (b) may result from a number of scattering mechanisms which are not individually resolved in the spectrum shown in Fig. 3. Such inelastic processes could be the excitation of X-point longitudinal acoustic (LA), transverse optical (TO), and longitudinal optical (LO) phonons, for example. The experimental and theoretical J–V curves presented in Figs. 2 and 4 are in good agreement.

Another possible way for electrons to tunnel through the AlAs band gap at the X point arises from the coupling of AlAs X-point states to GaAs Γ-point states due to the breaking of translational symmetry in the direction perpendicular to the layers. This makes it possible for Γ-point electrons in one GaAs electrode to tunnel elastically through the AlAs X-point barrier into Γ-point states in the other GaAs electrode. In this process, the virtual X-point states to consider are those below the two X valleys lying along the k_x direction, perpendicular to the plane of the layers. Since electrons travel along the x axis, the effective mass of importance in the barrier is the large longitudinal effective mass $m_l^* = 1.1m_e$. Preliminary calculations indicate that the coupling of states having different symmetries in GaAs and AlAs may be significant in the heterostuctures studied and could yield current densities large enough to account for the discrepancies observed between experimental and Γ-point elastic tunneling currents.

We have proposed two separate mechanisms by which Γ-point electrons in the GaAs electrodes may tunnel through the AlAs X-point barrier. In fact, both processes may occur simultaneously, and the empirical factors used to calculate theoretical current densities can be modified accordingly. More detailed calculations of scattering matrix elements and the mixing of states of different symmetry are under way to obtain a quantitative picture of electron transport in these structures. Nevertheless, the preliminary results presented here suggest that (i) elastic tunneling through the AlAs Γ-point barrier is insufficient to account for experimental current densities; (ii) elastic and inelastic tunneling through the AlAs band gap at the X point could account for the observed discrepancies; and (iii) theoretical current densities in good agreement with experimental data can be obtained provided both Γ- and X-point tunneling contributions are taken into account.

Although these concepts have only been illustrated in terms of the experimental data related to one structure, it was found that samples having different doping concentrations and barrier thicknesses display the same general behavior. Nevertheless, further investigations are necessary to gain a better understanding of the specific mechanisms occurring in each sample and to build a unifying model for all of them. This work will be discussed more thoroughly in a forthcoming publication.

IV. IMPURITY-ASSISTED TUNNELING

In this section, a new element is added to the current density calculations, namely the effect of impurity energy levels in the AlAs band gap. Impurity atoms and crystal defects can create localized energy levels (traps) in the AlAs barrier.[19,20] If these "impurity states" lie in the AlAs band gap, they can affect tunneling currents through the structure. In this paper, we view traps as intermediate states through which two-step tunneling processes may occur: an electron first tunnels from one GaAs electrode to an intermediate state, and then from the intermediate state to the other electrode. This approach is similar to that used by Parker and Mead in their treatment of traps in Schottky barriers.[21]

A simple expression for the two-step tunneling current can be derived by assuming that there are N localized trap states per unit volume of AlAs, with each trap energy level, E_i, being a fixed energy, E_o, below the AlAs conduction band edge, E_c. For an arbitrary voltage applied to the structure, the AlAs conduction band edge and thus the trap energy level vary with position, x:

$$E_i(x) = E_c(x) - E_o \,. \tag{1}$$

In Fig. 5, this concept is illustrated by plotting the Γ-point conduction band edge and a trap energy level for a single p-type barrier heterostructure under applied bias. This figure is the result of a band bending calculation, in which the electrode and barrier dopings are taken to be 3×10^{18} and 1×10^{18} cm^{-3}, respectively. The barrier thickness is 100 Å and the applied voltage is 150 mV. The impurity level is

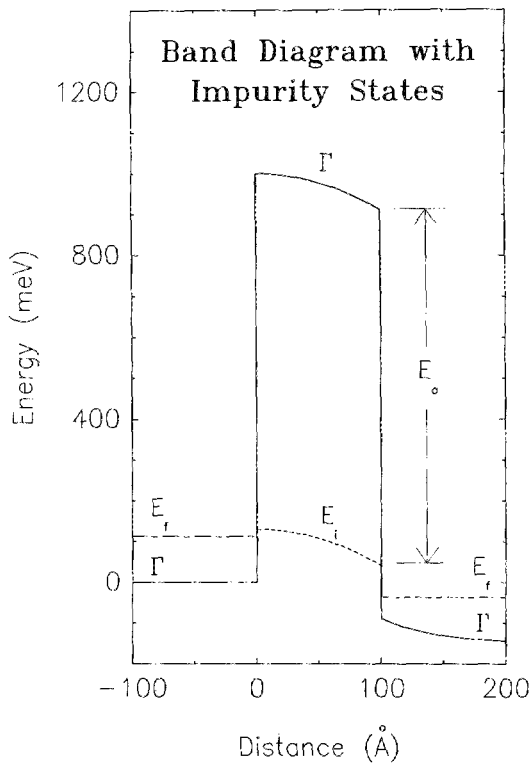

FIG. 5. Calculated Γ-point conduction band edge (solid line) as a function of distance in the direction perpendicular to the layers for a GaAs–AlAs–GaAs single barrier structure having an impurity level in the AlAs barrier layer. The impurity state (dashed line) lies 870 meV below the Γ-point conduction band edge in the barrier. The GaAs electrodes are doped n-type at 3×10^{18} cm^{-3}. The AlAs barrier layer is 100 Å thick, and doped p-type at 1×10^{18} cm^{-3}. A voltage of 150 mV is applied to the structure.

taken to be 870 meV below the AlAs Γ-point conduction band edge.

The elastic tunneling current density, J_1, between a trap state at position x_o and the left GaAs electrode is of the form:

$$J_1 \propto T_1[E_i(x_o),x_o]\{f_l[E_i(x_o)] - F[E_i(x_o)]\}, \quad (2)$$

where T_1 is the WKB transmission probability for an electron with energy $E_i(x_o)$ tunneling from the left electrode to x_o, f_l is the occupation probability of the left electrode state with energy $E_i(x_o)$, and F is the occupation probability of the trap state. Similarly, the elastic tunneling current density, J_2, between the trap state at position x_o and the right electrode is given by:

$$J_2 \propto T_2[E_i(x_o),x_o]\{F[E_i(x_o)] - f_r[E_i(x_o)]\}, \quad (3)$$

where T_2 is the transmission probability for an electron with energy $E_i(x_o)$ tunneling from x_o to the right electrode, and f_r, is the occupation probability of the right electrode state with energy $E_i(x_o)$.

Under steady-state conditions, the trap level occupation probability, F, will adjust itself to make the two current densities equal. It follows that the impurity-assisted tunneling current, J_{imp}, takes the form:

$$J_{\text{imp}} = J_1 = J_2 \propto \frac{T_1T_2}{T_1+T_2}\{f_l[E_i(x_o)]\}. \quad (4)$$

A comparison of Eq. (4) with the usual expression for the one-step elastic tunneling current,[9] J_{el}, reveals that:

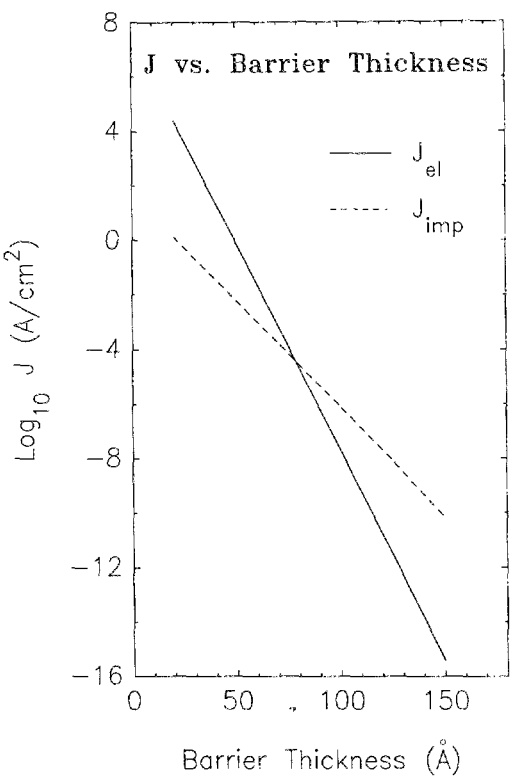

FIG. 6. Calculated current densities vs barrier thickness for one-step elastic tunneling (solid line) and impurity-assisted tunneling (dashed line). The dopings in the GaAs electrodes and the AlAs barrier are 3×10^{18} cm^{-3} and 1×10^{18} cm^{-3}, respectively. The applied voltage is 100 mV. The trap level is taken to lie 950 meV below the Γ-point conduction band edge in the barrier.

$$J_{\text{imp}} = C\,J_{\text{el}}\frac{1}{T_t(E_i)}\frac{T_1T_2}{T_1+T_2}, \quad (5)$$

where $T_t(E_i)$ is the transmission coefficient for electrons with energy E_i tunneling from the left electrode to the right electrode, and C is a constant which is proportional to the number of trap levels per unit volume, N, and the effective cross-sectional area of the traps, σ.

Figure 6 is a calculated plot of J_{imp} as a function of AlAs barrier thickness. The calculations are performed using a p-type barrier doping of 1×10^{18} cm^{-3}, and an n-type electrode doping of 3×10^{18} cm^{-3}. The applied voltage is 100 mV and the impurity energy level is taken to be 950 meV below the AlAs Γ-point conduction band edge. N is chosen to be 1×10^{17} cm^{-3}, and σ is assigned a value of ten times the cross-sectional area of the AlAs primitive cell. Changes in N and σ alter only the multiplicative constant, C, in Eq. (5), and therefore, do not change the qualitative behavior of J_{imp}. J_{el} is also calculated and plotted in Fig. 6 for comparison with J_{imp}. This reveals that the contribution to the total current density of one-step elastic tunneling is larger than that of impurity-assisted tunneling in heterostructures with thin barriers. The opposite is true in structures with thicker barriers. For the parameters used in Fig. 6, the impurity-assisted tunneling current becomes larger than the one-step elastic current when the AlAs barrier is thicker than about 80 Å.

V. IMPLICATIONS FOR RESONANT TUNNELING STRUCTURES

In this section, we briefly discuss implications of some of the previous results for resonant tunneling in GaAs/AlAs double barrier heterostructures. Resonant tunneling structures made of two $Al_xGa_{1-x}As$ quantum barriers separated by a GaAs quantum well display negative differential resistances in their I–V characteristics. This effect is commonly attributed to the tunneling of electrons via quasi-stationary states in the well. Furthermore, it is usually assumed that the effective barrier height for tunneling is determined by the Γ-point conduction band in the barriers, even when the $Al_xGa_{1-x}As$ is indirect. Detailed calculations of band bending, energy level positions, and voltage drops are required to determine without ambiguity, the correlation between the resonances in the well and the voltages at which negative differential resistances are observed. Simple theoretical models yield current densities in disagreement with experimental data. In structures for which the best peak-to-valley current ratios realized to date are 10:1 at 77 K,[22] calculations predict values as large as several orders of magnitude.[9] This indicates that the transport properties of these stuctures are more complex than simple models assess. In particular, the obtainable values of peak-to-valley current ratios are limited by other current transport mechanisms competing with Γ-point resonant tunneling.[23] Derivative spectra are important tools for identifying and investigating the nature of such processes. Figure 7 illustrates second derivative curves $(d^2I/dV^2)(V)$, obtained at 4.2 K for a resonant tunneling heterostructure. The GaAs electrodes in the sample are doped n-type with Se at 2×10^{18} cm^{-3}. The AlAs

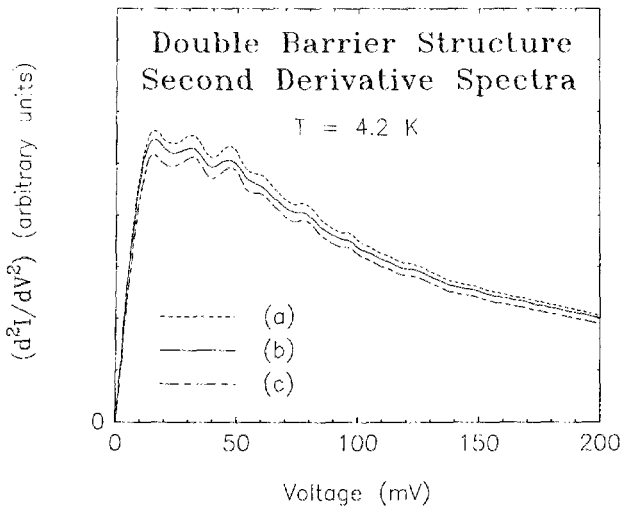

FIG. 7. Second derivative spectra $(d^2I/dV^2)(V)$, at 4.2 K for a GaAs/AlAs resonant tunneling double barrier heterostructure. The GaAs electrodes are doped n-type at 2×10^{18} cm^{-3}. The AlAs quantum barriers, approximately 50 Å thick, are doped p-type. The nominally undoped GaAs well is about 50 Å wide. The curves (a), (b), and (c) correspond to three different devices, having diameters of 145, 115, and 75 μm.

barriers, about 50 Å thick, are doped p-type with Mg. The nominally undoped GaAs well is about 50 Å wide. Three curves are shown in Fig. 7, corresponding to different size devices. They display reproducible features which have a nearly periodic spacing of 15–16 mV. Similar spectra are obtained from other samples. A definitive explanation of the observed features has not yet been found, but a possible interpretation may be proposed. The periodic structure could arise from the discrete nature of fluctuations in the quantum well width. Such fluctuations in barrier and well thicknesses would contribute in reducing and broadening the negative differential resistances observed in the I–V characteristics.

In the light of the results obtained for single barrier structures, it is possible to propose other qualitative explanations for the small peak-to-valley current ratios observed in several of our samples.[2] Whenever electrons can scatter to X-point states and tunnel through the AlAs barriers at the X point, a large background current can be expected, even for relatively thick barriers and wells. Depending upon the relative amplitudes of the resonant Γ-point current and the X-point current, the negative differential resistances may be partially or totally suppressed. Determining whether or not this will happen is, in fact, a nontrivial problem which depends upon the structure parameters and scattering mechanisms. In single barrier samples, electrons may tunnel through the AlAs band gap at the X point either inelastically by scattering near each interface, or elastically through the coupling of AlAs X-point states and GaAs Γ-point states. In double barrier structures, the problem is different due to the presence of the GaAs well between the two AlAs barriers. At voltages which are low enough that the X-point conduction band edge in the GaAs well is higher in energy than the Fermi level in the left electrode, X-point tunneling may occur through several mechanisms. First, electrons may scatter once near each of the four GaAs/AlAs interfaces, thus tunneling through the AlAs barriers at the X point, but occupying states of Γ symmetry in the GaAs electrodes and well. Secondly, electrons may scatter only near the first and last GaAs/AlAs interfaces, thus tunneling in both barriers and the well through the X-point gaps of AlAs and GaAs. Finally, electrons may tunnel elastically due to the coupling of wave functions having different symmetries. Simple estimates have shown that the relative importance of these mechanisms depends on the well width, barrier thicknesses, and applied voltage. These processes either involve higher order mechanisms than those taking place in single barrier structures, or tunneling through thick X-point barriers consisting of the two AlAs barriers and the GaAs well. Therefore, their contribution can certainly be minimized by carefully optimizing the structure parameters, improving the quality of the interfaces, and lowering the background doping in nominally undoped layers.

VI. SUMMARY

The objective of this study was to investigate elastic and inelastic tunneling processes in GaAs–AlAs–GaAs double heterojunctions grown by MOCVD in the [100] direction. The AlAs quantum barriers in the heterostructures studied were doped p-type with Mg. Measurements of current–voltage characteristics (I–V), as well as first (dI/dV) and second (d^2I/dV^2) derivatives of the I–V curves, were performed at temperatures ranging from 300 to 4.2 K. Experimental and theoretical results indicated that low temperature electron transport in structures with thin barriers is achieved through two mechanisms: (i)elastic electron tunneling through the AlAs Γ-point barrier; and (ii)inelastic and/or elastic tunneling through the AlAs X-point barrier. Inelastic X-point tunneling may occur via virtual states beneath the four X-point valleys lying parallel to the plane of the layers, and requires the scattering of electrons near each interface. Elastic X-point tunneling, due to the coupling of AlAs X-point states and GaAs Γ-point states, can take place via virtual states below the two AlAs X-point valleys lying in the direction perpendicular to the plane of the layers. A theoretical model, which treats trap levels in the AlAs barrier as intermediate states for two-step tunneling processes, was developed. Calculations indicated that this impurity-assisted tunneling mechanism can become important when the AlAs barrier is thick enough. Implications of some of these results for resonant tunneling heterostructures consisting of two AlAs quantum barriers separated by a GaAs quantum well were discussed. In particular, carefully choosing the parameters of these structures to maximize the contribution of the Γ-point resonant tunneling current is critical for increasing the peak-to-valley current ratios of the negative differential resistances. For these double barrier structures, we also presented experimental second derivative spectra (d^2I/dV^2), in which periodic features may be indicative of discrete fluctuations in well thickness.

ACKNOWLEDGMENTS

The authors wish to acknowledge R. S. Bauer, C. Mailhiot, R. H. Hauenstein, R. H. Miles, T. K. Woodward, and

G. Y. Wu for valuable discussions, and are grateful to H. F. Chung, F. Endicott, D. M. Taylor, T. T. Tjoe, T. Anderson, J. Tramontana, W. Mosby, D. W. Treat, and F. E. Nelson for technical assistance. This work was supported in part by the Defense Advanced Research Agency under Contract No. N000014-84-C-0083 and the Office of Naval Research under Contract No. N00014-82-K-0556.

[1]R. T. Collins, J. Lambe, T. C. McGill, and R. D. Burnham, Appl. Phys. Lett. **44**, 532 (1984).
[2]A. R. Bonnefoi, R. T. Collins, T. C. McGill, R. D. Burnham, and F. A. Ponce, Appl. Phys. Lett. **46**, 285 (1985).
[3]I. Hase, H. Kawai, K. Kaneko, and N. Watanabe, Electron. Lett. **20**, 491 (1984).
[4]L. L. Chang, L. Esaki, and R. Tsu, Appl. Phys. Lett. **24**, 593 (1974).
[5]D. Delagebeaudeuf, P. Delescluse, P. Etienne, J. Massies, M. Laviron, J. Chaplart, and N. T. Linh, Electron. Lett. **18**, 85 (1982).
[6]P. Guéret and U. Kaufmann, Electron. Lett. **21**, 344 (1985).
[7]T. C. L. G. Sollner, W. D. Goodhue, P. E. Tannenwald, C. D. Parker, and D. D. Peck, Appl. Phys. Lett. **43**, 588 (1983).
[8]M. A. Reed, Superlattices and Microstructures (1986).
[9]R. Tsu and L. Esaki, Appl. Phys. Lett. **22**, 562 (1973).
[10]B. Jogai and K. L. Wang, Appl. Phys. Lett. **46**, 167 (1985).
[11]H. M. Manasevit, Appl. Phys. Lett. **12**, 156 (1968).
[12]R. D. Dupuis and P. D. Dapkus, Appl. Phys. Lett. **31**, 466 (1977).
[13]C. R. Lewis, W. T. Dietze, and M. J. Ludowise, Electron. Lett. **18**, 569 (1982).
[14]R. D. Burnham, W. Streifer, D. R. Scifres, C. Lindstrom, T. L. Paoli, and N. Holonyak, Electron. Lett. **18**, 1095 (1982).
[15]G. C. Osbourn, J. Vac. Sci. Technol. **17**, 1104 (1980).
[16]C. Mailhiot and T. C. McGill, J. Vac. Sci. Technol. B **1**, 637 (1983).
[17]E. O. Kane, *Physics of III–V Compounds* (Academic, New York, 1966), Vol. 1, Chap. 3, pp. 75–100.
[18]J. Batey and S. L. Wright, J. Appl. Phys. **59**, 200 (1986).
[19]T. K. Woodward, T. E. Schlesinger, T. C. McGill, and R. D. Burnham, Appl. Phys. Lett. **47**, 631 (1985).
[20]H. P. Hjalmarson, Superlattices and Microstructures **1**, 379 (1985).
[21]G. H. Parker and C. A. Mead, Appl. Phys. Lett. **14**, 21 (1969).
[22]M. A. Reed (private communication).
[23]G. Y. Wu, A. R. Bonnefoi, and T. C. McGill (to be published).